

part and several side branches. Group  $\eta$  is mixed with the bands of the main sequence around  $\lambda 4140$ ; it seems to have a quite complicated structure. All the bands given in Table X are either too weak or insufficiently resolved or hopelessly overlapped by other bands and require reinvestigation with a much more powerful and purer spectral light source and at least equally high dispersion. It can be expected that a successful analysis of all the weaker band systems described in Part IV, and of the more complicated bands, will lead to a deeper understanding of the electronic spectrum of a triatomic molecule.

In conclusion I should like to express my

sincere thanks to Professor R. S. Mulliken for his continued interest in this work and to Professor H. D. Smyth for putting kindly at my disposal unpublished data and photographs of the spectrum of  $\text{CO}_2^+$  obtained by him some time ago with a 21-foot grating spectrograph. The careful study of these photographs revealed very good agreement with my results; the higher purity of the spectrum obtained by Professor H. D. Smyth was an important factor in strengthening my confidence in the correctness of the results reported in this and the preceding paper. I am also very much indebted to Mr. T. J. Kinyon for assistance in computations.

## The Conservation of Momentum in the Disintegration of $\text{Li}^8$

R. F. CHRISTY, E. R. COHEN, W. A. FOWLER, C. C. LAURITSEN, and T. LAURITSEN  
*Kellogg Radiation Laboratory, California Institute of Technology, Pasadena, California*  
 (Received July 11, 1947)

Apparatus for the introduction of radioactive materials into a cloud chamber has been employed to investigate the conservation of momentum in the  $\beta$ -decay of  $\text{Li}^8$  to  $\text{Be}^8$ , which subsequently breaks up into two  $\alpha$ -particles. The projection on the plane of measurement of the angle between the two  $\alpha$ -particles is a measure of one component of the recoil momentum of the  $\text{Be}^8$ . Additional information is obtainable from the momentum of the electron but relatively few cases occur where both  $\alpha$ -particles and the electron are in the plane of the cloud chamber. The  $\text{Li}^8$  is produced by bombarding with deuterons a thin deposit of  $\text{LiOH}$  on beryllium or gold foils. The mean squares of the observed momenta relative to the maximum possible momenta were 0.247 (Be foil) and 0.349 (Au foil). Corrected for scattering and other errors these become  $0.197 \pm 0.025$  and  $0.207 \pm 0.034$ , respectively, the probable errors quoted being statistical in origin. The weighted mean, rounded off to two figures, is  $0.20 \pm 0.02$ . This value is roughly twice that obtained taking into account only the emitted electrons, and approximately equal to that calculated for an electron and neutrino emitted with no preferred angle of ejection between them.

### 1. INTRODUCTION

THE conservation of momentum in the disintegration of radioactive nuclei by electron and positron emission and by the capture of electrons from extra-nuclear levels has been the subject of numerous experimental investigations.<sup>1-5</sup> These investigations have generally

<sup>1</sup> A. I. Leipunski, Proc. Camb. Phil. Soc. **32**, 301 (1936).

<sup>2</sup> H. R. Crane and J. Halpern, Phys. Rev. **56**, 232 (1939).

<sup>3</sup> L. W. Alvarez, A. C. Helmholtz, and B. T. Wright, Phys. Rev. **60**, 160 (1941); B. T. Wright, *ibid.* **71**, 839 (1947).

<sup>4</sup> J. S. Allen, Phys. Rev. **61**, 692 (1942).

<sup>5</sup> J. C. Jacobsen and O. Kofoed-Hansen, D. Kgl. Danske Vidensk. Selskab Mat.-fys. Medd **23**, 12 (1945).

consisted in measuring the energy of the recoiling daughter nucleus either by counting the number of ions formed as the nucleus is brought to rest in a gas or by determining the retarding potential necessary to bring the nucleus to rest in vacuum. As the atomic weight of the daughter nucleus is usually known, its momentum can be calculated and compared with that to be expected theoretically. These experiments have shown that the maximum momentum of the recoiling nucleus is equal to that to be expected from the maximum observed energy of the emitted electron or positron but that the momentum of recoil is

greater, on the average, than that of the electron or positron. Furthermore, nuclear recoil has even been observed in the capture of extra-nuclear electrons, Allen<sup>4</sup> having observed and measured such a recoil in the disintegration of  $\text{Be}^7$ .

The results are consistent with the suggestion made by Pauli that a neutrino is emitted in these disintegrations. If the neutrino be assumed to have an energy given by the amount available in the transition between the mother and daughter nucleus minus that of the electron and the small energy of the recoiling nucleus, and if it is also assumed to have very small rest mass, its momentum can be computed. This suggestion, coupled with Fermi's<sup>6</sup> assumptions concerning the distribution in momentum between electron and neutrino, is sufficient to account for the observed distributions in momenta of the recoiling nuclei although the quantitative agreement has not been nearly as exact as in the determination of the maximum momentum. Perhaps the most critical tests are those of Jacobsen and Kofoed-Hansen<sup>5</sup> who found by means of retarding potentials a distribution in the momenta of daughter nuclei from the decay of  $\text{Kr}^{88}$  which was not consistent with the recoil from the decay electrons alone, and which even indicated qualitatively that the neutrino is emitted in this particular disintegration mainly in the same direction as the electron.

The disintegration of  $\text{Li}^8$  by electron emission<sup>7</sup> is unique in that it is followed by the breakup of the daughter nucleus,\*  $\text{Be}^8$  into two alpha-particles.<sup>8-10</sup> The initial electron decay has a half-life of 0.88 second<sup>11</sup> and is followed by the alpha-particle decay in a time of the order of  $10^{-21}$  second as indicated by the spread (uncer-

tainty) in the alpha-particle energies.<sup>9,12-14</sup> The  $\text{Be}^8$  nucleus is probably formed in one of several broad excited states extending up to 12 Mev in excitation. The observed energy spectrum of the emitted electrons extends at least to  $12.0 \pm 0.6$  Mev and has been shown to be consistent<sup>15,16</sup> with the energy spectrum of the alpha-particles and with the fact that approximately 16.0 Mev is available in the complete transition from  $\text{Li}^8$  to two alpha-particles. The mass of  $\text{Li}^8$  is determined from the threshold bombarding energy<sup>12</sup> ( $\sim 0.2$  Mev) in the reaction  $\text{Li}^7 + \text{H}^2 \rightarrow \text{Li}^8 + \text{H}^1$ .

In a coordinate system moving with the center of mass of the two alpha-particles the momenta of the alpha-particles are equal and oppositely directed. In laboratory coordinates the motion of this mass center will be observable in that there will be, in general, a small deviation from  $180^\circ$  in the angle between the two alpha-particles and in that the momenta, and hence energies and ranges of the two particles, will not, in general, be identical. These effects will be discussed quantitatively below but at this point it will suffice to note their orders of magnitude. The recoil momentum of the  $\text{Be}^8$  will be at most the maximum electron energy divided by the velocity of light:

$$p_r \leq E_{\text{max}}/c, \quad (1)$$

giving  $5 \times 10^7$  cm/sec. for the maximum value of the recoil velocity,  $v_r$ . The velocity of the alpha-particles,  $v_\alpha$ , in the center of mass system is approximately  $10^9$  cm per sec. for the decay of the 3.0-Mev excited state in  $\text{Be}^8$ , so that the angular deviation from  $180^\circ$  in the angle between the two alpha-particles in laboratory coordinates is

$$\theta \sim 2 \frac{v_r}{v_\alpha} \sin \varphi \leq 2 \frac{v_r}{v_\alpha} \leq \frac{1}{10} \text{ radian or } 6^\circ, \quad (2)$$

where  $\varphi$  is the angle between the recoil of the  $\text{Be}^8$  and its line of breakup in the center of mass system. For a given amount of recoil the maximum deviation from  $180^\circ$  occurs when the  $\text{Be}^8$

<sup>6</sup> E. Fermi, Zeits. f. Physik **88**, 161 (1934).

<sup>7</sup> H. R. Crane, L. A. Delsasso, W. A. Fowler, and C. C. Lauritsen, Phys. Rev. **47**, 971 (1935); L. H. Rumbaugh and L. R. Hafstad, Phys. Rev. **50**, 681 (1936).

\* Throughout this paper the formation of  $\text{Be}^8$  as an intermediate stage in the ultimate decay of  $\text{Li}^8$  into two alpha-particles will be assumed. This has been done primarily for convenience in discussing the disintegration. Considerations regarding the conservation of energy and momentum in the over-all process are independent of any assumptions concerning intermediate stages.

<sup>8</sup> P. I. Dee and C. W. Gilbert, Proc. Roy. Soc. **A154**, 279 (1936).

<sup>9</sup> W. A. Fowler and C. C. Lauritsen, Phys. Rev. **51**, 1103 (1937).

<sup>10</sup> E. Wigner and G. Breit, Phys. Rev. **50**, 1191 (1936); G. Breit and E. Wigner, Phys. Rev. **51**, 593 (1937).

<sup>11</sup> W. B. Lewis, W. E. Burcham, and W. Y. Chang, Nature **139**, 24 (1937).

<sup>12</sup> L. H. Rumbaugh, R. B. Roberts, and L. R. Hafstad, Phys. Rev. **51**, 1106 (1937) and **54**, 657 (1938).

<sup>13</sup> C. Smith and W. Y. Chang, Proc. Roy. Soc. **A166**, 415 (1938).

<sup>14</sup> T. W. Bonner, Phys. Rev. **72**, 163 (1947).

<sup>15</sup> D. S. Bayley and H. R. Crane, Phys. Rev. **52**, 604 (1937).

<sup>16</sup> Charles Kittel, Phys. Rev. **55**, 515 (1939).

breaks up in a plane normal to its direction of recoil. When the  $\text{Be}^8$  breaks up parallel to its direction of recoil the maximum difference in velocity and range of the two alpha-particles occurs. For the velocity difference we have:

$$\Delta v_\alpha \sim 2v_r \cos\phi \leq 2v_r. \quad (3)$$

For low energy alpha-particles the range varies approximately as the square of the velocity so that

$$\frac{\Delta R_\alpha}{R_\alpha} \sim 2 \frac{\Delta v_\alpha}{v_\alpha} \sim 4 \frac{v_r}{v_\alpha} \cos\phi \leq 4 \frac{v_r}{v_\alpha} \leq 20 \text{ percent.} \quad (4)$$

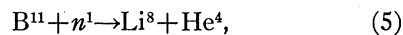
Hence range differences of as much as 20 percent and angular deviations from  $180^\circ$  of as much as  $6^\circ$  are to be expected.

It is the purpose of this paper to describe experiments in which cloud-chamber photographs of the beta-decay of  $\text{Li}^8$  and the subsequent alpha-particle breakup of  $\text{Be}^8$  have been obtained.\*\* In a few cases photographs in which all three particles lie in the plane of the cloud chamber have been obtained and some analysis of these photographs has been attempted. In the main, however, emphasis has been placed on those more numerous photographs in which only the two alpha-particles occurred in such locations as to make measurements possible. Attempts were made to determine in general the deviation of the angle between the two alphas from  $180^\circ$  and the difference in their ranges. Scattering and loss of energy of the alpha-particles in the target in which the  $\text{Li}^8$  was produced and in the gas of the cloud chamber introduced errors into these determinations. Uncertainty in the energy losses was such as to preclude the possibility of accurate determinations from the observed range differences, while the scattering corrections were found to introduce mean errors of the order of 25 percent in the determination of the angle. The most reliable information is believed to be that determined from the angular deviations measured on tracks in which the range differences were at most that to be expected

\*\* It has come to our attention that numerous investigators have proposed the study of the conservation of momentum in the decay of  $\text{Li}^8$  and we are grateful in particular to Doctor E. R. Gaertner, Professor H. R. Crane, and Professor Nicholas Feather for correspondence on the subject.

from Eq. (4). Measurements of the projection of this angle on a vertical plane were not attempted for reasons described below, and so these measurements in principle are concerned with the determination of one component in a Cartesian coordinate system of the recoil momentum of the  $\text{Be}^8$ . In most cases this component lay in a horizontal plane. In those cases where measurements on the electron as well as on the alpha-particles could be obtained it was possible to specify one component of the resultant momentum of the three observable particles. Any component should of course be zero if momentum is conserved among these particles. However, all other cases could be treated only on a statistical basis by employing Fermi's equation for the distribution in momenta of the electrons.

Attempts to obtain cloud-chamber photographs of both the beta- and alpha-disintegrations of  $\text{Li}^8$  were first made in this laboratory in 1937 at about the same time that the alpha-radioactivity was under investigation.<sup>9</sup> In a method devised by H. R. Crane, a small pump was utilized to transfer into a cloud chamber a sample of gas which contained recoils from a lithium target bombarded by deuterons. In a second method a lithium target was mounted on a stopcock in such a way that it could be rapidly rotated into a cloud chamber after bombardment in vacuum. Neither of these attempts was successful, the reason for the most part being that the cloud chamber was usually fogged by small amounts of impurities or by ionized gases introduced into it during the operations. No experiments on this problem were carried out during the war years and it was not until late in 1945 that a new attack was started. It was believed that the most promising line of attack would be to produce  $\text{Li}^8$  directly in the cloud chamber by neutron irradiation, and the reaction first chosen was

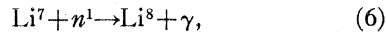


as it has been shown<sup>17</sup> that  $\text{Li}^8$  is produced by fast neutrons in this way. Boron was introduced into the chamber in the form of methyl borate\*\*\* and it was found possible to obtain a large

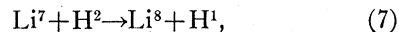
<sup>17</sup> A. M. Lawrance, Proc. Camb. Phil. Soc. 35, 304 (1939).

\*\*\* We are grateful to Professor H. J. Lucas and Mr. C. N. Scully who prepared the methyl borate used in these experiments.

number of tracks in the chamber gas which corresponded to the disintegration<sup>18</sup> of B<sup>10</sup> by slow neutrons to form Li<sup>7</sup> and He<sup>4</sup>. No evidence for the formation of Li<sup>8</sup> was found, however, and it was concluded that the cross section for this reaction must be very small. A second reaction was also tried, namely,



but again no activity could be detected in agreement with the small cross section ( $10^{-27}$  cm<sup>2</sup>) for this reaction which has been recently measured.<sup>19</sup> It was finally decided to produce the Li<sup>8</sup> by bombardment of Li<sup>7</sup> by deuterons according to the reaction



and to attempt again to transfer the Li<sup>8</sup> into the chamber. This was done successfully in the manner described below. Preliminary results<sup>20</sup> of these experiments were first reported at the Stanford meeting of the American Physical Society in July, 1947.

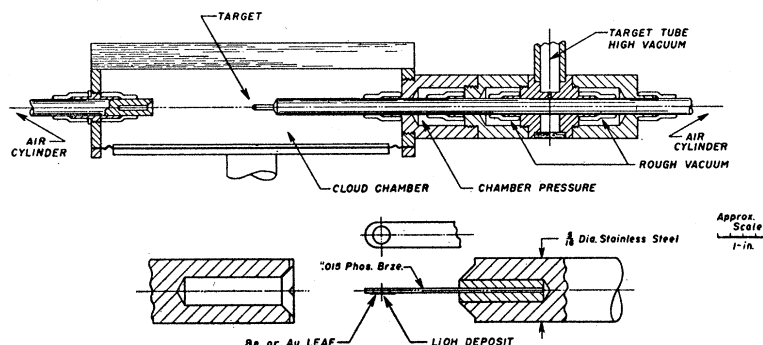
## 2. EXPERIMENTAL ARRANGEMENT

The Li<sup>8</sup> was produced by bombardment of a LiOH target by 1-Mev deuterons from the electrostatic generator, previously described.<sup>21</sup> After bombardment of the target for about 0.5 second, the target was introduced into the cloud chamber by the automatic mechanism shown in Fig. 1. The target is mounted at the end of a  $\frac{5}{16}$ " diameter stainless-steel rod which, with an inter-

locking extension rod, passes through a series of locks connecting the bombardment position and the cloud chamber. Immediately after bombardment of the target, an air cylinder advances the target rod, pushing the target into a socket in the end of the extension rod and passing the assembly successively through a rough vacuum region, a region at cloud-chamber pressure, and into the cloud chamber. Once the target is in the cloud chamber, a second air cylinder retracts the extension rod, exposing the target. A rotation of one and one-quarter turns is provided by a helix in the advancing air cylinder to facilitate passage through the seals and to present the target in the proper orientation in the cloud chamber. When the target is in the center of the chamber, the chamber is expanded and a photograph taken. The sheath is then advanced to cover the target and the assembly is passed back through the locks and opened in the bombarding position. Seals between the locks are provided by Koroseal sleeves lubricated with stopcock grease. The elapsed time for a 10" motion of the target into the cloud chamber is about 1.5 seconds with a somewhat longer interval allowed on the return stroke to permit pumping out in the rough vacuum lock. The entire cycle is repeated every 45 seconds.

The target material was sprayed from a LiOH solution to a just visible thickness (usually in the form of partially coalesced droplets) on a backing of gold leaf (0.176 mg/cm<sup>2</sup> or  $\sim 10^{-5}$  cm) or of beryllium foil\*\*\*\* (0.092 mg/cm<sup>2</sup> or  $\sim 5 \times 10^{-5}$  cm)

FIG. 1. Apparatus for the introduction of short-lived radioactivity into a cloud chamber.



<sup>18</sup> J. K. Bøggild, D. Kgl. Danske Vidensk. Selskab Mat.-fys. Medd **23**, 4 (1945).

<sup>19</sup> M. J. Poole and E. B. Paul, Nature **158**, 482 (1946).

<sup>20</sup> W. A. Fowler, C. C. Lauritsen, and T. Lauritsen, Phys. Rev. **72**, 738(A) (1947).

<sup>21</sup> T. Lauritsen, C. C. Lauritsen, and W. A. Fowler, Phys. Rev. **59**, 241 (1941).

\*\*\*\* We are indebted to Dr. Hugh Bradner of the Radiation Laboratory of the University of California for the beryllium foils.

which was mounted over a 2.5-mm hole in a light phosphor bronze strip attached to the sliding rod. Quite frequent replacement of targets was necessitated by the deposition of oil films from the lubricant. The stopping power of the foil and target is estimated to be equivalent to approximately 1 mm of standard air or 2 to 3 mm of the gas-vapor mixture used in the chamber.

The cloud chamber was filled with helium gas. In the gold-foil measurements the chamber also contained vapor in equilibrium with a liquid mixture of 65 percent ethyl alcohol and 35 percent water. The total pressure was 0.9 atmospheres in the expanded position so that the calculated stopping power<sup>22</sup> for 2-Mev alpha-particles was 0.267. In the beryllium-foil measurements the vapor was in equilibrium with a liquid mixture of equal parts of ethyl and methyl alcohol. The total pressure was 1.5 atmospheres so that the stopping power was 0.447. The variation of stopping power with energy was taken into account.<sup>22</sup> The stopping-power calculations were checked satisfactorily by measuring on the photographs the range of alpha-particles from a polonium source located at one side of the chamber. An aluminum foil of 1.8-cm air equivalence reduced the lengths of the tracks from the polonium so that they terminated in the chamber. The ranges were measured to the nearest half-millimeter and were thus known to approximately 0.2 mm in standard range. Errors in energy measurement from this source were less than 2 percent.

Turbulence near the target and loss of pressure was largely avoided by holding the final lock at the same pressure as the chamber, allowing the cavity in the sheath rod to fill before passing into the chamber. The best tracks were obtained by using a fast expansion and by providing ample time (45 seconds) to clear between expansions. The sweep field was intensified by two fine wires strung across the top glass. A magnetic field of 2300 gauss was used in the beryllium-foil measurements and fields of 1700 and 2300 gauss were used at different times in the gold-foil measurements.

### 3. MEASUREMENTS

Photography was accomplished by two Sept cameras, one located directly above the chamber and one set off at 18° from the vertical. The off-vertical camera was used solely in the preliminary observations for determining stereoscopically the orientation of the various tracks in space. In reprojection through the original negatives, with the same cameras and mounts, it was possible to locate points in a vertical plane to within one or two millimeters. However, in most cases the angle between the alpha-particles differed so little from 180° that their actual plane could not be determined. Hence photographs of usable tracks were printed on a tilting stage adjusted to lie in a plane containing the mean line of the alpha-particle pair and a horizontal line at right angles to this mean line. Photographs in which electron tracks could be associated with an alpha-particle pair were printed in the plane containing the initial direction of the electron (tangent to the curved path arising from the magnetic field) and the mean line of the alphas. Prints were made in this way only of the negative obtained by the camera mounted directly above the chamber.

The angle between the alpha-pairs was measured on the prints by means of a vernier protractor and it is believed that the limit of error was  $\pm 0.5^\circ$ . For the most part the tracks were not visible within 7.5 mm (3-mm standard range) of the target support. In the angle measurements the portions of the tracks nearest the support were bisected by fine lines drawn on the prints and the angle between the extension of these lines measured. In this way the effect of large angle scatterings near the end of the tracks was eliminated.

It will be noted that angle measurements as described here do not yield the actual angle between the two alpha-particles since only the projection of this angle on the print is obtained and the projection on a vertical plane is completely neglected. In the photographic method employed in which one camera was directly above the cloud chamber and the other nearly so, practically no information about the projection on a vertical plane is obtained for small angles. It was felt that more elaborate photographic techniques employed to measure this projection would not

<sup>22</sup> M. S. Livingston and H. A. Bethe, *Rev. Mod. Phys.* **9**, 271 (1937).

have yielded useful results. The reason for this is the fact that the motion of the gas in the chamber during the expansion is largely vertical, and so some distortion in the vertical plane arises from the presence of the target support. A downward displacement of the end of tracks relative to the portion near the target is to be expected except for tracks of particles entering after completion of the expansion. Measurements were confined to tracks showing little diffusion of droplets in order to minimize this and other distortions, but it was not felt that measurements of the vertical projection could be made in a trustworthy manner.

Approximately 10,000 cloud-chamber photographs were taken during these experiments and photographs of about 500 pairs were printed after preliminary inspection of the projected images. In further selection after the prints were available about 200 pairs were rejected for one or more of the following reasons:

- (1) The tracks were diffused, distorted, or exhibited large scatterings.
- (2) The tracks passed out of the light beam near the end of their range.
- (3) One of the tracks lay within  $30^\circ$  of the axis of the metal rod supporting the target and thus had possibly been subject to distortions arising from the flow of gas around this rod.

(4) The mean line through the pair made an angle greater than  $30^\circ$  with the horizontal.

(5) More than two pairs appeared on the photograph making association of the proper pair members somewhat uncertain. There was little doubt in most cases as to which tracks were to be associated in pairs, but it was felt wise not to employ photographs on which the existence of more than two pairs made association in principle uncertain.

Among the remaining 300 pairs it was found that about 30 percent showed range differences which were too large to be ascribed to the maximum possible recoil of the  $\text{Be}^8$ , while only about 10 percent showed angles too large to be ascribed to this recoil. The appearance on some photographs of single alpha-particle tracks indicated there were two possible explanations for the large range differences. In the first place, the single tracks indicated that pair members could be stopped in the  $\text{LiOH}$  target or in the supporting foils. Hence some large energy differences were to be expected where one pair member suffered a considerable energy loss but not enough to be completely stopped. This was felt to be the main explanation of the observed range differences. In the second place, apparent pairing of two tracks, each of which had lost its true pair member, could occur accidentally although this was clearly rather improbable. In any case it was not felt that the range differences gave a reliable

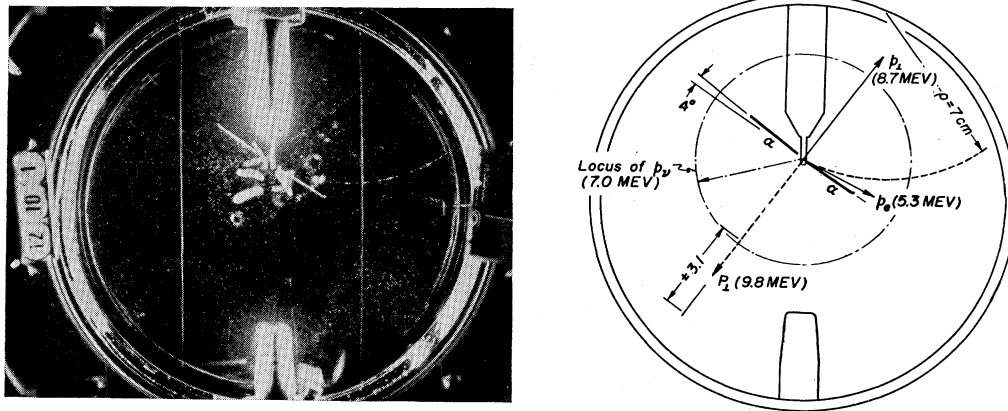


FIG. 2. Film No. 95062. The sharp alpha tracks and the electron track are assumed to arise from the decay of a single  $\text{Li}^8$  nucleus produced in the target. A line extending roughly from the upper left hand corner to the lower right can be drawn in such a way that the momentum vectors of all three particles lie to the right of it. The resultant momentum of the three particles is  $9.8 \pm 3.1$  in Mev units where the uncertainty arises from the possibility of scattering of the alpha-particles. A neutrino with the remaining available energy of 7.0 Mev (16.0 Mev minus the alpha and electron energies) could have this momentum within the probable error. The magnetic field was directed upward. The electron and neutrino momenta are designated by  $p_e$  and  $p_\nu$ , respectively. The momentum of the alpha-particles normal to their mean line of break-up in the plane of the print is  $p_\perp$ . The resultant momentum of the alpha-particles and the electron is  $P_L$  (shown in opposite direction in the figure).

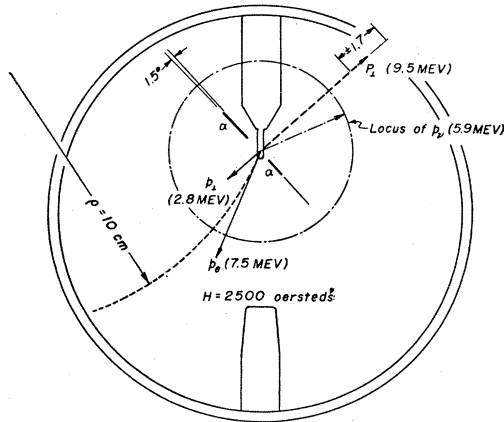
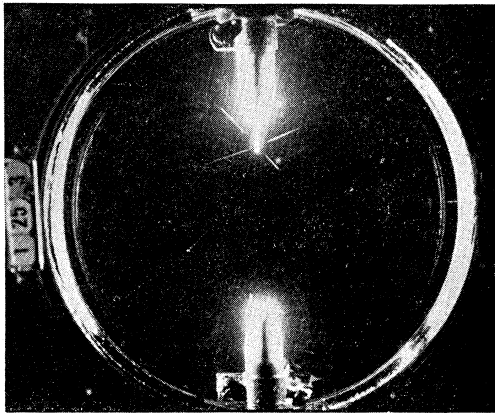


FIG. 3. Film No. 97952. This photograph is illustrative of the difficulty arising in cases where more than one alpha-pair occurred on the same film. In this instance the members of one pair pass out of the illuminated portion of the chamber and thus cannot be used for quantitative measurements. The assumption that the electron is associated with the other pair leads to a resultant momentum of the observable particles greater than that which can be had by a neutrino with the remaining energy. The magnetic field was directed downward.

measurement of the recoil, and it did not seem that the measurement of angles between tracks showing large differences in range was acceptable. For this reason the final analysis of results was confined to the angular measurements on those pairs which did not differ in range by an amount more than that to be expected from the maximum possible recoil of the  $\text{Be}^8$ . This criterion resulted in the final acceptance of 130 pairs in the photographs obtained using the beryllium foils and 87 pairs on photographs obtained using gold foils.

In 28 cases it was found possible to associate measurable electron tracks with the alpha-particle pairs. This number is considered reasonable in view of the small probability of an electron track lying close enough to the horizontal plane to remain in the illuminated portion of the chamber for a distance comparable to its radius of curvature. On these photographs the orientation of the tangent to the electron track with one member of the alpha-pair was measured. The radii of curvature of the electron tracks were measured in projection on a horizontal plane (normal to the magnetic field). The momentum of the electron is proportional to the product of this radius with the known value of the field and hence it and the energy can be simply computed.

#### 4. ANALYSIS OF THE MEASUREMENTS

##### (a) Alpha-Particle Pairs with Electrons

Reproductions of photographs showing electrons and pairs of alpha-particles are shown in

Figs. 2-4. It will be recalled that these photographs were printed in a plane containing the initial direction of the electron and the mean line of the alpha-particles. Photographs were only made in those cases in which this plane did not make an angle of more than  $35^\circ$  with the horizontal plane and in which the plane of the electron track itself did not make an angle of more than  $10^\circ$  with the horizontal. A graphical analysis of each case is shown with each reproduction. In each analysis we have computed the component of the momentum of the electron normal to the mean line of the alpha-particles and lying in the plane of the print. The electron path is not exactly a circle in these prints and so the radii of curvature were measured in separate projections on the horizontal plane. In addition we have computed the recoil momentum of the  $\text{Be}^8$  as indicated by the angle between the alpha-particles as measured on the print. This momentum is also the component normal to the mean line of the alpha-particles lying in the plane of the print. It is obtained from the angle and observed range of the alpha-particles by first determining the mean velocity  $\bar{v}_\alpha$  of the two alphas, using the range-velocity relation for the gas-vapor mixture as calibrated with alphas from the polonium source. In part (b) of this section it is shown that the momentum is given by

$$p_\perp = M_\alpha \theta \bar{v}_\alpha, \quad (8)$$

where  $\theta$  is the deviation from  $180^\circ$  of the angle

between the two alpha-particles. By adding this algebraically to the corresponding component of the momentum of the electron,  $p_{\perp}(e)$ , we obtain  $P_{\perp}$ , the resultant momentum of the three observable particles normal to the mean line of the alpha-particles and lying in the plane of the alphas and electron. We have compared this with the possible total momentum of a neutrino of zero rest mass which has an energy given by 16 Mev minus the observed energy of the two alpha-particles and the electron. This total momentum of the neutrino should not be less than any one component of the resultant momentum of the observed particles. We have indicated the probable error of this resultant momentum because it is the least accurately determined quantity due primarily to the large probabilities of scattering of the alpha-particles (see final section). Twenty-eight cases in all have been analyzed and are tabulated in Table I. The association of electron tracks with alpha-particles is in some cases doubtful because of the appearance of other alpha-particles on the same picture. In addition the selection criteria in these cases were considerably relaxed compared to those used in the statistical study of alpha-particle pairs in Section (b) below. In Fig. 2, for example, these are many diffuse alpha-particle tracks which apparently entered the cloud chamber some time before the photograph was

TABLE I. Analysis of photographs showing electrons and alpha-particle pairs. Components of momentum normal to  $\text{Be}^8$  breakup.

| Film number    | $E_{\alpha}$<br>Mev | $\theta$<br>degrees | $E_e$<br>Mev | $p_{\perp}$<br>Mev | $p_{\perp}(e)$<br>Mev | $P_{\perp}$<br>Mev | $E_{\nu}=p_{\nu}$<br>Mev |
|----------------|---------------------|---------------------|--------------|--------------------|-----------------------|--------------------|--------------------------|
| Beryllium foil |                     |                     |              |                    |                       |                    |                          |
| 97338          | 5.0                 | 0.5                 | 5.1          | -1.2               | 2.8                   | $1.6 \pm 1.3$      | 5.9                      |
| 97688          | 3.5                 | 0.0                 | 5.2          | 0.0                | 0.0                   | $0.0 \pm 1.6$      | 7.3                      |
| 97952          | 3.1                 | 1.5                 | 7.0          | 2.8                | 6.7                   | $9.5 \pm 1.7$      | 5.9                      |
| 97959          | 4.1                 | 1.5                 | 5.5          | 3.2                | 6.0                   | $9.2 \pm 1.5$      | 6.4                      |
| 97995          | 2.3                 | 2.9                 | 7.1          | 4.7                | 7.6                   | $12.3 \pm 2.0$     | 6.6                      |
| 98001          | 4.8                 | 1.7                 | 4.8          | -3.9               | 4.1                   | $0.2 \pm 1.4$      | 6.4                      |
| 98002          | 4.2                 | 2.0                 | 6.3          | 4.4                | 0.5                   | $4.9 \pm 1.5$      | 5.5                      |
| 98041          | 3.2                 | 2.6                 | 8.2          | 4.9                | 0.0                   | $4.9 \pm 1.7$      | 4.6                      |
| 98092          | 6.1                 | 6.0                 | 0.8          | 15.8               | -1.2                  | $14.6 \pm 1.2$     | 9.1                      |
| 98145          | 3.5                 | 2.7                 | 6.3          | 5.4                | -1.5                  | $3.9 \pm 1.6$      | 6.2                      |
| 98244          | 4.5                 | 5.0                 | 6.3          | 11.3               | -5.9                  | $5.4 \pm 1.5$      | 5.2                      |
| 98312          | 3.1                 | 1.1                 | 7.8          | 2.0                | 8.1                   | $10.1 \pm 1.7$     | 5.1                      |
| 98490          | 5.3                 | 2.0                 | 7.1          | 4.9                | 1.8                   | $6.7 \pm 1.3$      | 3.6                      |
| 98588          | 6.6                 | 1.3                 | 3.7          | 3.6                | -2.9                  | $0.7 \pm 1.2$      | 5.7                      |
| 98623          | 5.9                 | 2.6                 | 5.9          | 6.9                | -6.4                  | $0.5 \pm 1.2$      | 4.2                      |
| 98634          | 2.8                 | 2.9                 | 5.6          | -5.2               | 6.0                   | $0.8 \pm 1.8$      | 7.6                      |
| Gold foil      |                     |                     |              |                    |                       |                    |                          |
| 91551          | 2.8                 | 0.9                 | 6.3          | 1.7                | -1.1                  | $0.6 \pm 3.8$      | 6.9                      |
| 91603          | 4.5                 | 2.8                 | 9.2          | 6.3                | -0.3                  | $6.0 \pm 3.0$      | 2.3                      |
| 91644          | 5.1                 | 3.3                 | 4.1          | 8.1                | -2.6                  | $5.5 \pm 2.8$      | 6.8                      |
| 91811          | 2.7                 | 7.1                 | 8.6          | 12.4               | -6.4                  | $6.0 \pm 3.9$      | 4.7                      |
| 94734          | 1.9                 | 1.3                 | 7.1          | -2.0               | 7.6                   | $5.6 \pm 4.6$      | 7.0                      |
| 94899          | 5.2                 | 1.5                 | 3.7          | -3.7               | 4.2                   | $0.5 \pm 2.8$      | 7.1                      |
| 95046          | 4.3                 | 2.0                 | 3.3          | 4.4                | -2.6                  | $1.8 \pm 3.1$      | 8.4                      |
| 95060          | 2.7                 | 6.3                 | 5.9          | 11.1               | -5.4                  | $5.7 \pm 3.9$      | 7.4                      |
| 95062          | 4.2                 | 4.0                 | 4.8          | 8.7                | 1.1                   | $9.8 \pm 3.1$      | 7.0                      |
| 95063          | 1.9                 | 1.6                 | 3.7          | 2.1                | 3.7                   | $5.8 \pm 4.6$      | 10.4                     |
| 95282          | 1.5                 | 8.5                 | 3.7          | 11.6               | 4.0                   | $15.6 \pm 5.2$     | 10.8                     |
| 95478          | 4.6                 | 2.0                 | 6.3          | 4.6                | 5.0                   | $9.6 \pm 3.1$      | 5.1                      |

taken. It is argued that electrons associated with these tracks would also be diffuse and thus not

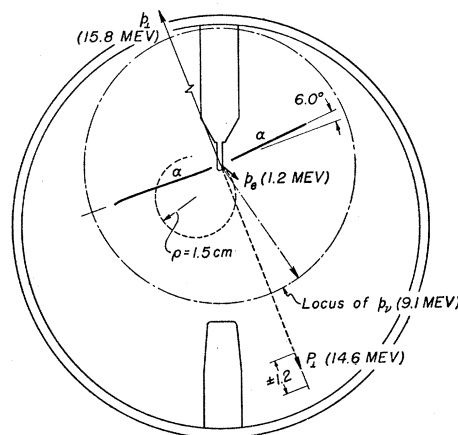
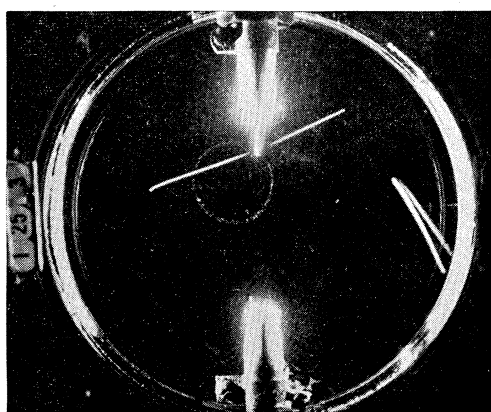


FIG. 4. Film No. 98092. In this photograph the angle between the two alpha-particles deviates by  $6^\circ$  from  $180^\circ$ . This cannot be caused by recoil from the low energy electron also appearing. On the other hand, the expected scattering is only about  $\frac{1}{2}^\circ$ . Recoil from a neutrino with the available energy will account for an angle of about  $4^\circ$  and the remainder can be attributed to a scattering several times that to be expected on the average. The difference in range of the two alphas indicates that the right-hand particle has suffered a large energy loss, probably in an unusually thick part of the target. The magnetic field was directed downward.



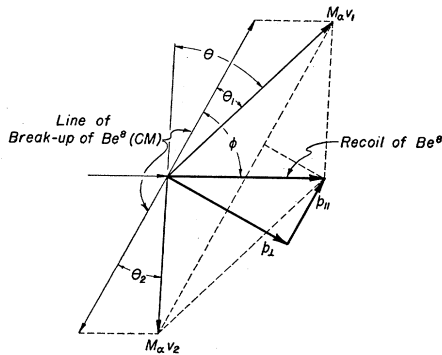


FIG. 5. Analysis of the resultant momentum of the two alpha-particles. The angle  $\theta = \theta_1 + \theta_2$  is in general much smaller than the angle  $\varphi$ . *CM* indicates the center of mass system.

in general visible and that the electron is most probably the one associated with the sharp pair. At one time in the experiments, shutters were mounted on either side of the target position in the chamber and were opened by the piston motion only at the end of the expansion. These were found to introduce considerable turbulence and to scatter considerable light into the camera and so were eventually discarded. In Fig. 3 the situation is even worse since a sharp pair which passed almost vertically through the chamber, each member leaving the illuminated region, occurs on the photograph in addition to the pair used in the measurements. The analysis was made in this case solely to determine if the neutrino hypothesis was consistent with the assumption that the electron was associated with the pair used in the measurements. In Fig. 4 these difficulties do not occur. In this photograph the angle between the alpha-particles is more than twelve times that to be expected from scattering or from recoil from the observed low energy electron.

An examination of the data on these 28 pictures shows that in the majority of cases the observed resultant momentum of alpha-particles and electron is much larger than can be accounted for by scattering alone. In many of these cases the momentum can be understood on the neutrino hypothesis although in some the resultant momentum is larger than can be explained on the assumption that the electron and neutrino have no preferred angle of emission. As a result, although there is observed an unbalanced

momentum such as would be given by a neutrino, the data are not sufficient for a meaningful numerical comparison with any definite assumption concerning the angular distribution of electron and neutrino.

(b) Alpha-particle Pairs without Electrons

In cases where it is not possible to associate electrons with the alpha-particle pairs it is still useful to make an analysis of the resultant momentum of the two alpha-particles in laboratory coordinates. This resultant momentum can be resolved into components parallel and perpendicular to the line of breakup of the alphas in a system moving with their center of mass. From Fig. 5 we have

$$p_{\perp} = M_{\alpha}v_1 \sin\theta_1 + M_{\alpha}v_2 \sin\theta_2, \quad (9)$$

$$p_{\parallel} = M_{\alpha}v_1 \cos\theta_1 - M_{\alpha}v_2 \cos\theta_2, \quad (10)$$

where  $\theta_1$  and  $\theta_2$  are the angles between the velocity of the alpha-particles in the center of mass coordinates and their velocity in laboratory coordinates. The velocities in laboratory coordinates are  $v_1$  and  $v_2$ . The velocities of alpha-disintegration are in all observable cases large compared to the recoil velocities. Hence  $v_1$  and  $v_2$  are approximately equal as are  $\theta_1$  and  $\theta_2$ . Then, in terms of the average velocity  $\bar{v}_{\alpha} = \frac{1}{2}(v_1 + v_2)$  and the velocity difference  $\Delta v_{\alpha} = v_1 - v_2$ , we have

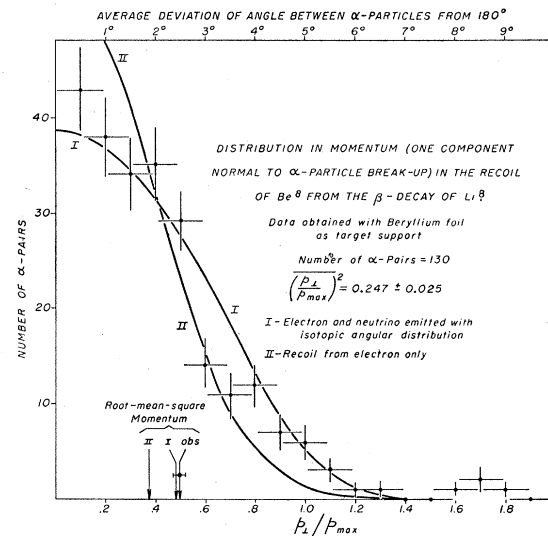


FIG. 6. Distribution in  $p_{\perp}/p_{\max}$  for 130 alpha-pairs obtained with a beryllium foil for target support.

Eq. (8) which was employed above:

$$p_{\perp} = M_{\alpha} \bar{v}_{\alpha} \theta,$$

where

$$\theta = \theta_1 + \theta_2. \quad (11)$$

We also have

$$p_{\parallel} = M_{\alpha} \Delta v_{\alpha}. \quad (12)$$

In terms of the energy of the two alpha-particles  $E_{\alpha} = E_1 + E_2$  and the energy difference  $\Delta E_{\alpha} = E_1 - E_2$  we have

$$p_{\perp} = \theta (M_{\alpha} E_{\alpha})^{\frac{1}{2}} = 1.07 E_{\alpha}^{\frac{1}{2}} \theta \quad (13)$$

and

$$p_{\parallel} = \Delta E_{\alpha} (M_{\alpha} / E_{\alpha})^{\frac{1}{2}} = 61 E_{\alpha}^{-\frac{1}{2}} \Delta E_{\alpha}, \quad (14)$$

where in the numerical expressions, energies and momenta† are in Mev and angles in degrees. The maximum resultant momentum of the two alpha-particles can be computed from the maximum energy available in the electron-neutrino decay. This will be the total energy  $Q$  available in the disintegration of  $\text{Li}^8$  minus the disintegration energy of the alpha-particles. We have

$$p_{\max} = (Q - E_{\alpha}) / c, \quad (15)$$

where  $Q$  is 16.0 Mev. We normalize the two

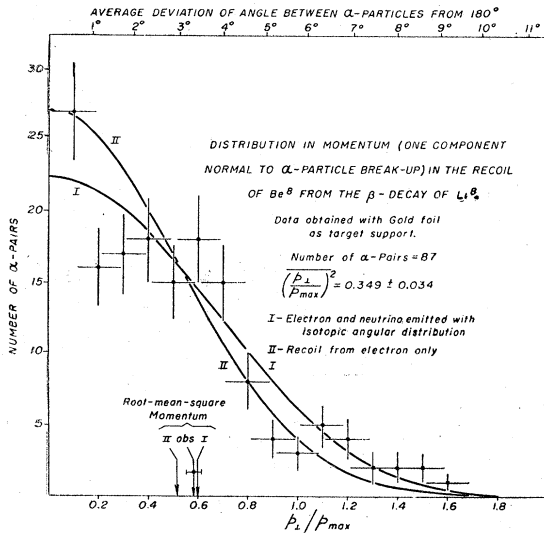


FIG. 7. Distribution in  $p_{\perp}/p_{\max}$  for 87 alpha-pairs obtained with a gold foil for target support.

† The convenient energy unit, the Mev, can be used for momenta if the momenta are always considered to be multiplied by the velocity of light.

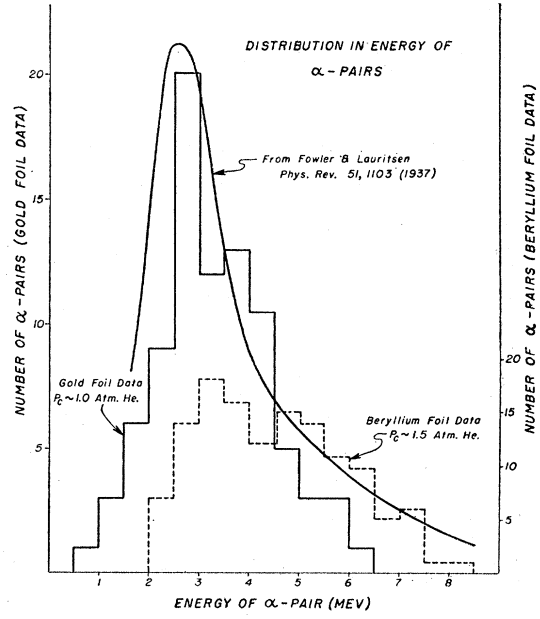


FIG. 8. Distribution in energy of the alpha-pairs employed in these measurements with the distribution in energy of all pairs from  $\text{Li}^8$  shown for comparison.

components of momentum to this value so that

$$\begin{aligned} \frac{p_{\perp}}{p_{\max}} &= \frac{M_{\alpha} c^2 \bar{v}_{\alpha}}{Q - E_{\alpha}} \frac{(M_{\alpha} c^2 E_{\alpha})^{\frac{1}{2}}}{Q - E_{\alpha}} \theta \\ &= 1.07 \frac{E_{\alpha}^{\frac{1}{2}}}{16 - E_{\alpha}} \theta, \end{aligned} \quad (16)$$

and

$$\begin{aligned} \frac{p_{\parallel}}{p_{\max}} &= \frac{M_{\alpha} c^2 \Delta v_{\alpha}}{Q - E_{\alpha}} \frac{(M_{\alpha} c^2 / E_{\alpha})^{\frac{1}{2}}}{Q - E_{\alpha}} \Delta E_{\alpha} \\ &= 61 \frac{\Delta E_{\alpha}}{E_{\alpha}^{\frac{1}{2}} (16 - E_{\alpha})}. \end{aligned} \quad (17)$$

These expressions were employed in analyzing about 300 alpha-particle pairs. As discussed above, all those cases for which  $p_{\parallel}/p_{\max} > 1$  were excluded from the final analysis. These final results are shown in Figs. 6 and 7 in which are plotted the number of alpha-particle pairs having specified values of  $p_{\perp}/p_{\max}$ . The distribution in energy of the pairs included in these measurements is shown in Fig. 8. The distribution in energy of all the alpha-pairs from  $\text{Li}^8$  as originally measured by Fowler and Lauritsen<sup>9</sup> is also shown for comparison. Since the projection on a vertical plane of the angle between the two

TABLE II. Calculated momentum distribution and mean-square momenta.

| Neutrino distribution                     | Distribution of $\perp$ component of recoil momentum $p_{\perp}$  | $\langle p_{\perp}^2 \rangle_{Av}$ | $\langle p^2 \rangle_{Av}$ |
|---|---|------------------------------------|----------------------------|
| Neutrino anti-parallel to electron        | $\frac{15}{8} \left[ \ln \frac{1}{p_{\perp}} - \frac{1}{4} (1 - p_{\perp}^2) (3 - p_{\perp}^2) \right]$ | $\frac{1}{21}$                     | $\frac{1}{7}$              |
| Recoil from electron only                 | $\frac{5}{2} (1 - p_{\perp})^3 (1 + 3p_{\perp})$  | $\frac{2}{21}$                     | $\frac{2}{7}$              |
| $\Theta(\theta) = 1 + \alpha \cos \theta$ | $\frac{5}{16} (1 - p_{\perp}^2) \left[ (5 - \alpha) - (1 - 5\alpha) p_{\perp}^2 \right]$                | $\frac{4 + \alpha}{21}$            | $\frac{4 + \alpha}{7}$     |
| Neutrino parallel to electron             | 1   | $\frac{7}{21}$                     | 1                          |

alpha-particles was not determined in these measurements the  $p_{\perp}$  actually calculated for each pair is only one component of the resultant momentum normal to the line of breakup. The relation between this component and the angle as measured on the photographs is the same as given in Eq. (16) above.

## 5. CALCULATIONS

### (a) Recoil Momentum Distributions

The distribution of recoil momentum of the excited  $\text{Be}^8$  nucleus will depend on the momentum (or energy) distribution of the electrons and if the existence of the Pauli neutrino is supposed, on the relative angular distribution of electron and neutrino. The over-all electron energy distribution was measured directly<sup>15</sup> and was found to be consistent with the supposition that, associated with each observed alpha-particle pair there is an electron-neutrino pair with total energy equal to  $16 \text{ Mev} - E_{\alpha}$  and distributed in energy according to the simple Fermi distribution. The existence of a copious gamma-ray following the beta-decay is ruled out by the above energy considerations. Furthermore, delayed gamma-rays have been looked for<sup>12,15</sup> without success. Consequently, in what follows we shall suppose that all the energy not appearing in the alpha-pair is distributed between electron and neutrino with a Fermi distribution. Since this energy is usually large compared to  $mc^2$ , we shall equate  $E$  for the electron to  $pc$ . We also assume that all beta-transitions have the same characteristics, i.e., they correspond to transitions to the same type of excited state of

$\text{Be}^8$ . This is made plausible by the apparent absence of irregularities in the final alpha-spectrum but is particularly justified in this experiment where almost all the alpha-pairs have an energy corresponding to the disintegration of a single broad excited state of  $\text{Be}^8$  at about 3 Mev. With the above assumptions we are able to normalize the recoil momentum of  $\text{Be}^8$  in each disintegration to the maximum recoil available from parallel electron and neutrino. Writing all momenta in these units we have the momentum of  $\text{Be}^8$  given by

$$p^2 = p_e^2 + p_{\nu}^2 + 2p_e p_{\nu} \cos \theta, \quad (18)$$

where  $\theta$  is the angle between  $\mathbf{p}_e$  and  $\mathbf{p}_{\nu}$ . The probability distribution of  $p_e, p_{\nu}$  is given by

$$W(p_e) dp_e = 30 p_e^2 (1 - p_e)^2 dp_e. \quad (19)$$

For the angular distribution of electron and neutrino we take

$$\Theta(\theta) d\theta = \frac{1}{2} (1 + \alpha \cos \theta) \sin \theta d\theta, \quad (20)$$

where, with  $p_e c \approx E_e$ ,  $\alpha$  may take on values from  $-1$  to  $1$  and in particular<sup>23</sup> takes the values  $-1, 1, \frac{1}{3}, -\frac{1}{3}, -1$ , respectively, for the simple scalar, polar vector, tensor, axial vector, and pseudo-scalar allowed interactions. With the above and  $p_{\nu} = 1 - p_e$ , we obtain the probability distribution of  $\text{Be}^8$  momentum recoil

$$P(p) dp = (5/4) p^2 [3(1 - \alpha) - (1 - 5\alpha) p^2] dp. \quad (21)$$

In addition we consider two limiting angular distributions:  $p_{\nu}$  parallel to  $p_e$  or  $\theta = 0$ .

$$P(p) dp = \delta(1 - p) dp \quad (22)$$

<sup>23</sup> D. R. Hamilton, Phys. Rev. **71**, 456 (1947).

where  $\delta$  is the delta-function of the argument  $(1-p)$  and  $p_\nu$  antiparallel to  $p_e$  or  $\theta=180^\circ$ .

$$P(p)dp = (15/8)(1-p^2)^2 dp. \quad (23)$$

Finally we consider the case  $p_\nu=0$  (recoil due to electron only) but retain (19) as an observed fact

$$P(p)dp = 30p^2(1-p)^2 dp. \quad (24)$$

As already indicated, the observations of the  $\text{Be}^8$  momentum are restricted to a single component normal to the direction of its disintegration into two alpha-particles. We must then know the disintegration probability of the  $\text{Be}^8$  as a function of the angle between  $\mathbf{p}$  and the direction of the alphas. This can only be known by knowing the initial state of  $\text{Li}^8$ , the beta-decay coupling, and the final state of  $\text{Be}^8$ , none of which is known for sure. According to the most probable description of these transitions, however, the disintegration probability of  $\text{Be}^8$  will be independent of the relative directions of alpha-particles and recoil. We have used this "symmetry of breakup of  $\text{Be}^8$ " assumption in calculating the distribution of component momentum.

According to Wheeler,<sup>24</sup> the excited state of  $\text{Be}^8$  involved here is not the  $J=0$  state found in  $\alpha-\alpha$  scattering at 3 Mev, which would, of course, lead to symmetry in the breakup of the  $\text{Be}^8$ . On the contrary, it is probably described as  $^1D_2$  and the ground state of  $\text{Li}^8$  as  $^3P_2$ .<sup>25</sup> As Konopinski<sup>26</sup> points out, the beta-transition to the  $^1D_2$  state is then of the allowed type but unfavored since it proceeds by means of the non-conservation of orbital angular momentum. The symmetry of breakup of  $\text{Be}^8$  then follows from the fact that the electron and neutrino are emitted in an S state since the first term in the expansion of  $\exp[(i/\hbar)(\mathbf{p}_e + \mathbf{p}_\nu) \cdot \mathbf{r}]$  is responsible for the transition. The transition to the ground state of  $\text{Be}^8$  is doubly forbidden by the parity-angular momentum-selection rules.

It is to be noted that the formation of  $\text{Li}^8$  by deuteron bombardment on  $\text{Li}^7$  presumably involves a change in parity, and since it is a threshold reaction, this probably means that it is only the  $p$ -wave deuterons that are effective,

the low energy emitted protons being  $s$  wave. This should show up in any careful analysis of the excitation function for the reaction which has not, however, been attempted here.

The assumption of spherical breakup thus appears more probable than any other definite assumption we could make. The probability distributions of a single component of the recoil momentum of  $\text{Be}^8$  is then easily made giving the distributions and average squares of  $p_\perp$ , the component of  $p$  in Table II and Fig. 9. It is to be noted that  $\langle p_\perp^2 \rangle_{\text{av}}$  is just  $\frac{1}{3} \langle p^2 \rangle_{\text{av}}$  for obvious reasons.

### (b) Corrections

In order to evaluate the correction to  $\langle p_\perp^2 \rangle_{\text{av}}$  arising from scattering, we need only  $\langle \theta^2 \rangle_{\text{av}}$ , the mean-square projected angle of Rutherford scattering. This is given, for small angles, by

$$\langle \theta^2 \rangle_{\text{av}} = \left( \frac{2Ze^2}{E} \right)^2 \pi N t \ln \frac{\theta_{\text{max}}}{\theta_{\text{min}}}, \quad (25)$$

where  $E$  is the energy of the alpha-particle and  $Z$ ,  $N$  the atomic number and number of particles/cc, respectively, of the scatterer. The

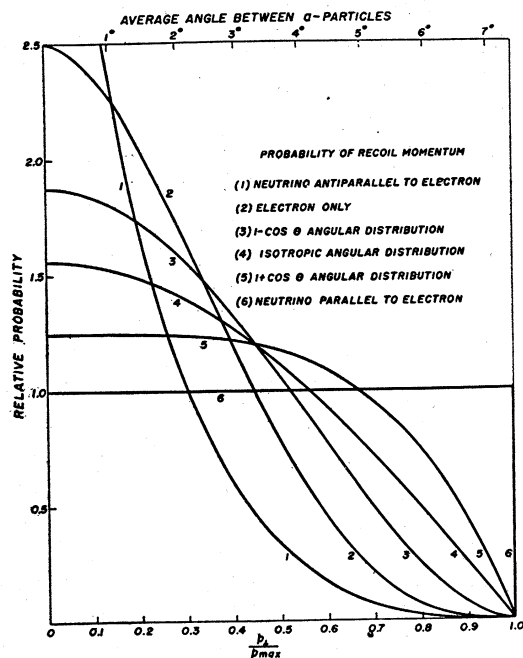


FIG. 9. Theoretical distributions of one component of the recoil momentum of  $\text{Be}^8$  for various angular orientations of electron and neutrino.

<sup>24</sup> J. A. Wheeler, Phys. Rev. **59**, 27 (1941).

<sup>25</sup> E. Feenberg and E. Wigner, Phys. Rev. **51**, 95 (1937).

<sup>26</sup> E. J. Konopinski, Rev. Mod. Phys. **15**, 209 (1943).

thickness,  $t$ , was taken to be the average foil path traversed by the alpha-particles which was 0.215 mg/cm<sup>2</sup> for the gold foil and 0.102 mg/cm<sup>2</sup> for the beryllium foil.  $\theta_{\max}$  is the maximum observed angle between two alpha-particles associated as a pair. This was 10° to 15° in this experiment.  $\theta_{\min}$  is a minimum angle of scattering determined by the electronic screening of the nuclear field. For 1-Mev alpha-particles in beryllium this may be taken to be  $\theta_{\min} = \lambda/a$  whereas in gold, the Born approximation is invalid and

$$\theta_{\min} \approx Ze^2/Ea \quad (26)$$

from the classical scattering calculation.  $a$  is the atomic radius given approximately by  $a_0 Z^{-1}$ . The scattering angle  $\langle \theta^2 \rangle_{\text{Av}}$  is related to the equivalent  $\Delta \langle p_{\perp}^2 \rangle_{\text{Av}}$  and is averaged over the energy distribution of the observed alpha-pairs to give the correction for scattering in the foil. The result is uncertain by about 20 percent for the gold foil because of approximations in the logarithm.

The correction for scattering in the cloud-chamber gas is handled similarly. In this case  $t$  was taken to be 1.3 cm—a measure of distance near the foil where the track was unobservable plus one-half the track length used to determine its direction.

A suitably averaged correction in  $\langle p_{\perp}^2 \rangle_{\text{Av}}$  was also introduced corresponding to an error of angular measurement of 0.5°.

The correction of the momentum distribution for scattering, etc., is in principle more difficult since it requires the use of a distribution in scattering angle. This could roughly be represented by a Gaussian distribution for small angles, with a width determined by  $\langle \theta^2 \rangle_{\text{Av}}$ , with  $\theta_{\max}$  the limit

of multiple scattering, and a single scattering tail. This calculation was performed however with a simple Gaussian distribution function of suitable width, so that the tail of the corrected distribution for  $p_{\perp} > 1$  may be somewhat underestimated.

It had been intended to obtain the component of momentum parallel to the alpha-particle direction from the difference in range of the two members of a pair. From the equality of the two components of  $p_{\perp}$  in the average, this would give  $\langle p^2 \rangle_{\text{Av}} = \langle p_{\parallel}^2 \rangle_{\text{Av}} + 2\langle p_{\perp}^2 \rangle_{\text{Av}}$  independent of the assumption of spherical breakup of Be<sup>8</sup>. The difference between  $\langle p_{\parallel}^2 \rangle_{\text{Av}}$  and  $\langle p_{\perp}^2 \rangle_{\text{Av}}$  would measure any asymmetry in this break up. The difference in range of the alphas would arise from penetration of the foil by one of them (known  $\approx 2$  mm of the chamber mixture), from straggling ( $\sim 0.4$  mm of chamber mixture), and from the actual difference in energy of the alphas. There resulted  $\langle p_{\parallel}^2 \rangle_{\text{Av}} \approx 0.8$  after subtracting the straggling correction of  $\sim 1$  percent. This led to  $\langle p^2 \rangle_{\text{Av}} > 1$  which is impossible. The cause of this result is uncertain but it might be due to accumulation of oil on the target or to thick spots of LiOH on the target. If it is explained in this manner it should be noted that the scattering corrections should be increased. However, if due to an element of atomic number about equal to that of carbon, the thickness represented by the observed range difference of about (4 mm) would only add 0.03 to the scattering correction. These data were actually used however to exclude certain tracks from measurement as discussed before. The resulting effect on  $\langle p_{\perp}^2 \rangle_{\text{Av}}$  was comparable to the estimate above. Furthermore if the observed  $p_{\parallel}$  were real, the large  $p_{\parallel}$  should mean small  $p_{\perp}$  and the exclusion should increase  $\langle p_{\perp}^2 \rangle_{\text{Av}}$ .

TABLE III. Mean-square momenta.

| Foil<br>Number of pairs  | Beryllium<br>130 | Gold<br>87    |
|--|------------------|---------------|
| Observed $\langle (p_{\perp}/p_{\max})^2 \rangle_{\text{Av}}$  | 0.247            | 0.349         |
| Corrections  |                  |               |
| Scattering in foil   | 0.006            | 0.110         |
| Scattering in gas  | 0.032            | 0.020         |
| Errors in measurement  | 0.012            | 0.012         |
| Total  | 0.050            | 0.142         |
| Corrected $\langle (p_{\perp}/p_{\max})^2 \rangle_{\text{Av}}$ | 0.197 ± 0.025    | 0.207 ± 0.034 |
| Weighted mean  | 0.20 ± 0.02      |               |

## 6. CONCLUSIONS

The theoretical distributions to be expected on the basis of various angular correlations of the electron and neutrino in the decay of the Li<sup>8</sup> are calculated in the preceding section. The distortion of the distributions due to scattering and errors in measurement is also calculated there. In Figs. 6 and 7 we include the results of these calculations giving corrections for two cases: I, recoil from the electron and neutrino emitted with no preferred orientation and II, recoil from

the electron only. It will be noted that the experimental points fit curve I slightly better than curve II but that the difference is by no means conclusive.

The best comparison with theory is made by comparing the observed mean-square values of  $p_{\perp}/p_{\max}$  with the theoretical values. In Table III are given the experimental values of  $\langle(p_{\perp}/p_{\max})^2\rangle_{Av}$  and the corrections as calculated in the previous section. The corrected experimental values are given with the probable errors listed being purely statistical in origin. It will be noted that the final result,  $\langle(p_{\perp}/p_{\max})^2\rangle_{Av} = 0.20 \pm 0.02$ , is slightly more than twice that to be expected from the recoil from the electron alone ( $2/21 = .095$ ). The theoretical considerations assume no correlation in the angle between the line of breakup of the Be<sup>8</sup> and the line of its recoil. Even if the Be<sup>8</sup> is assumed, as is unlikely, to breakup always in a direction normal to its recoil, the theoretical value is only three-quarters of the observed value. The result is not very selective with respect to the type of interaction in the Fermi theory, favoring, perhaps, the Tensor interaction, for which  $\alpha = \frac{1}{3}$ .

It will be noted that the corrections reduce the observed values by 20 percent and 40 percent in the beryllium-foil data and gold-foil data, respectively. Furthermore, the result of the exclusion of all pairs having  $p_{\perp}/p_{\max}$  greater than unity reduced the observed values of  $\langle(p_{\perp}/p_{\max})^2\rangle_{Av}$  by about 25 percent. These corrections are of course much larger than the statistical probable errors which have been quoted, and certainly make these

experiments a much less critical test of the neutrino hypothesis than is to be desired. On the other hand, the final result quoted contains all the corrections which we consider reasonable and we conclude that momentum is not conserved among the observable particles, alphas and electrons. On the other hand, the results seem not to violate the conservation of momentum if the emission of a neutrino is postulated and in particular if the neutrino emission shows no very preferred orientation with that of the electron. The experimental evidence supports this last point but by no means constitutes a conclusive proof of its validity. A more precise experimental determination and a more complete investigation of sources of error will be necessary before questions concerning the angular distribution in the electron-neutrino decay can be answered. The theoretical calculations given in Section 5 show that the recoils expected in the most extreme cases of forward or backward correlations, which are theoretically reasonable, differ only by 25 percent from the recoil expected in the case of no correlation. We have reduced our probable statistical errors to less than one-half of this difference but the scattering and selection corrections are of just this order of magnitude. Further data should be obtained from cloud-chamber photographs in which the Li is produced directly in the chamber gas and the scattering and loss of energy in target foils are avoided.

This work was carried on under contract with the Office of Naval Research.

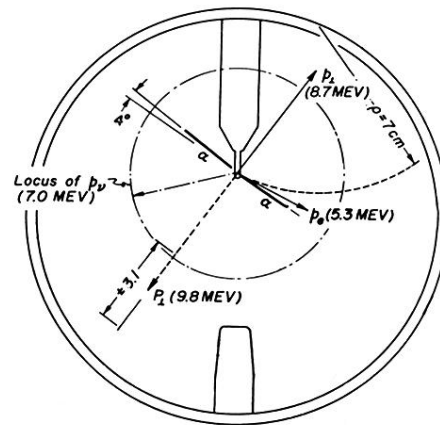
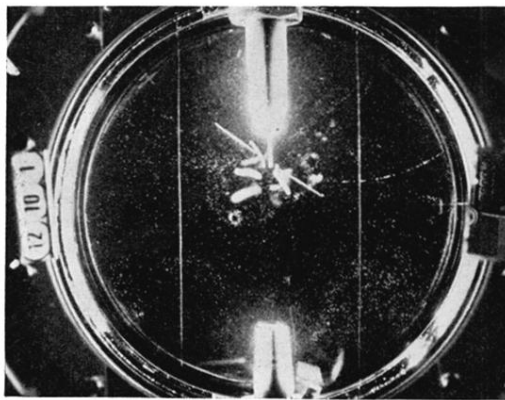


FIG. 2. Film No. 95062. The sharp alpha tracks and the electron track are assumed to arise from the decay of a single  $\text{Li}^8$  nucleus produced in the target. A line extending roughly from the upper left hand corner to the lower right can be drawn in such a way that the momentum vectors of all three particles lie to the right of it. The resultant momentum of the three particles is  $9.8 \pm 3.1$  in Mev units where the uncertainty arises from the possibility of scattering of the alpha-particles. A neutrino with the remaining available energy of 7.0 Mev (16.0 Mev minus the alpha and electron energies) could have this momentum within the probable error. The magnetic field was directed upward. The electron and neutrino momenta are designated by  $p_e$  and  $p_\nu$ , respectively. The momentum of the alpha-particles normal to their mean line of break-up in the plane of the print is  $p_\perp$ . The resultant momentum of the alpha-particles and the electron is  $P_\perp$  (shown in opposite direction in the figure).

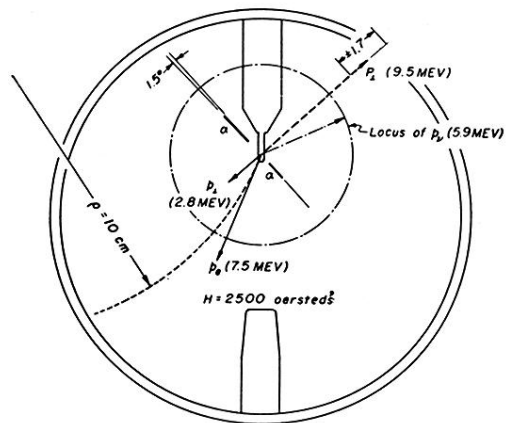
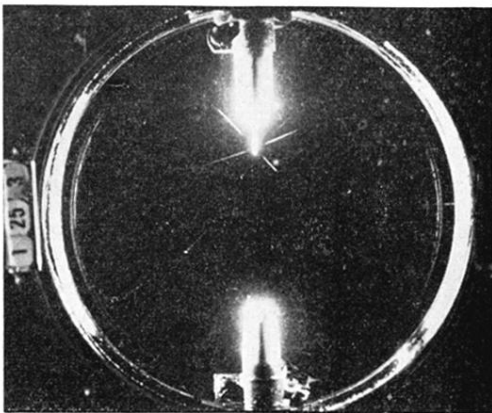


FIG. 3. Film No. 97952. This photograph is illustrative of the difficulty arising in cases where more than one alpha-pair occurred on the same film. In this instance the members of one pair pass out of the illuminated portion of the chamber and thus cannot be used for quantitative measurements. The assumption that the electron is associated with the other pair leads to a resultant momentum of the observable particles greater than that which can be had by a neutrino with the remaining energy. The magnetic field was directed downward.



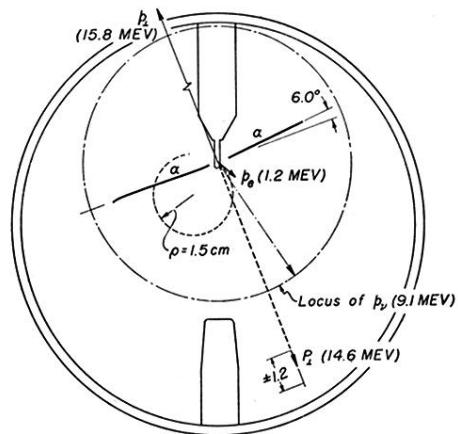
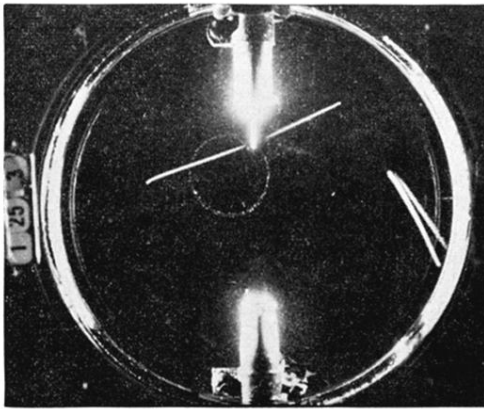


FIG. 4. Film No. 98092. In this photograph the angle between the two alpha-particles deviates by  $6^\circ$  from  $180^\circ$ . This cannot be caused by recoil from the low energy electron also appearing. On the other hand, the expected scattering is only about  $\frac{1}{2}^\circ$ . Recoil from a neutrino with the available energy will account for an angle of about  $4^\circ$  and the remainder can be attributed to a scattering several times that to be expected on the average. The difference in range of the two alphas indicates that the right-hand particle has suffered a large energy loss, probably in an unusually thick part of the target. The magnetic field was directed downward.